J. Dairy Sci. 107:9176–9196
https://doi.org/10.3168/jds.2023-24239

Nonlinear models of ^{15}N partitioning kinetics in late-lactation dairy cows from individually labeled feed ingredients

Kristan F. Reed,[1]* MaryGrace Erickson,[2] Tiago Barros,[2] Marina A. C. Danes,[3] J. Mark Powell,[4] Geoffrey I. Zanton,[4] and Michel A. Wattiaux[2]
[1]Department of Animal Science, Cornell University, Ithaca, NY 14850
[2]Department of Animal and Dairy Sciences, University of Wisconsin–Madison, Madison, WI 53705
[3]Department of Animal Science, University of Lavras, Lavras 37200, Brazil
[4]USDA-Agricultural Research Service, US Dairy Forage Research Center, Madison, WI 53705

ABSTRACT

Few studies have examined the N kinetics of individual feeds with stable isotope tracing. We hypothesized that N partitioning to milk and excreta pools as well as the rates of the processes that drive this partitioning would differ for alfalfa silage, corn silage, corn grain, and soybean meal. Feed ingredients were endogenously labeled with ^{15}N and included in 4 diets to create treatments with the same dietary composition and different labeled feed. Diets were fed to 12 late-lactation dairy cows for 4 d (96 h) and feces, urine, and milk collection proceeded during the 4 d of ^{15}N enrichment and for 3 d (80 h) after cessation of label feeding. Nonlinear models of ^{15}N enrichment and decay were fit to milk (MN), urine (UN), and fecal N (FN) in R with the nlme package, and feed-specific parameter estimates were compared. The estimated proportions of feed N that were excreted in feces supported our understanding that N from soybean meal and corn grain is more digestible than N from alfalfa and corn silage. Estimates for the N partitioning between milk and urine from the 2 concentrate feeds (soybean meal and corn grain) indicated that UN/MN ratios were less than or equal to 1:1, indicating either more or equal nitrogen partitioning to milk compared with urine. It is important to maintain factual accuracy in representing the results rather than implying a desired outcome unsupported by the data. In contrast, UN/MN ratios for forage feeds (corn and alfalfa silage) were >1:1, indicating more N partitioning to urine than milk. The modeled proportion of total FN that originated from feed N was 82.2%, which is in line with previous research using a similar ^{15}N measurement timeframe. However, the proportion of urinary and MN originating from feed N was much lower (60.5% for urine, 57.9% for milk), suggesting that approximately 40% of urinary and MN directly originate from body N sources related to protein turnover.

Key words: nitrogen, modeling, dairy cattle, isotope, tracer

INTRODUCTION

Losses of N from dairy farms contribute to a variety of environmental concerns, including GHG emissions, nitrate contamination of groundwater, and eutrophication of surface waters (Powell and Rotz, 2015). Ration formulation can modulate the efficiency of dietary N utilization and reduce N excretion in urine and feces. Urinary N (**UN**), in particular, increases linearly with dietary N content and is more labile than fecal N (**FN**), and thus is more easily lost to the environment (Dijkstra et al., 2013; Spek et al., 2013; Powell and Rotz, 2015). Dairy cattle nutrition models are often used to formulate diets and estimate dietary N use efficiency (i.e., milk N/intake N) and excretion. However, common nutrient requirement and excretion models are factorial, empirical models that provide minimal opportunity to evaluate the metabolism of the N from each feed ingredient and therefore its contribution to productive or unproductive fates (Reed et al., 2015; Barros et al., 2017; Powell et al., 2017). Elucidating the metabolic behavior of N from individual feedstuffs will improve our understanding of methods to achieve greater N efficiency, allowing for better assessment of whole farm N efficiency (Powell and Rotz, 2015; Powell et al., 2017). Tracing N from individual feedstuffs across metabolic processes enables a biophysical accounting of N inputs and N outputs in terms of environmental and economic impacts.

Dairy cattle nutrient requirement models also lack robust predictions of body protein contributions to N in milk, feces, and urine. Advancement in the contribution of endogenous animal protein to FN and thus to animal N requirements has been made (e.g., Lapierre et al., 2008; Marini et al., 2008; Lapierre et al., 2020), but little infor-

Received September 25, 2023.
Accepted May 9, 2024.
*Corresponding author: kfr3@cornell.edu

The list of standard abbreviations for JDS is available at adsa.org/jds-abbreviations-24. Nonstandard abbreviations are available in the Notes.

mation is available on body contributions to endogenous UN and milk protein. Therefore, a better understanding of the extent and kinetic nature of body protein cycling and contributions to milk and UN will improve the ability of nutrient requirement models to estimate N efficiency and excretion.

Stable isotope methods are uniquely suited to advancing our understanding of the mechanisms by which feed and body protein combine to form FN, UN, and milk N (**MN**) due to their ability to act as a tracer of specific N sources. The ^{15}N isotope has been used in a variety of ways to improve our understanding of dairy cattle N metabolism (e.g., Lapierre et al., 2008) and track N losses during manure storage and field application (Powell et al., 2005). Our group employed ^{15}N tracer methods in an interdisciplinary study to examine the effects of feed N source on N metabolism and partitioning in lactating cows, loss of ammonia and nitrous oxide from dairy barns and soils, and crop N uptake after labeled manure application to soil (Powell et al., 2017). Our preliminary analysis of N excretion data suggested the contribution of each feed to FN, UN, and MN varied, and that not all feed ^{15}N was recovered up to 80 h after cessation of label feeding (Barros et al., 2017). We hypothesized that in addition to differences between feeds in the partitioning to FN, UN, and MN, the dynamics of both digestion and metabolism that contribute to this partitioning are also specific to each feed. To further elucidate and quantify the distinct behavior of N excretion between feeds, we applied nonlinear modeling techniques to the ^{15}N excretion data and hypothesized that the kinetics of N metabolism, in addition to the partitioning between feces, urine, and milk, would vary among feeds.

MATERIALS AND METHODS

Experimental plots within larger fields of alfalfa (**AS**) and corn for silage (**CS**), corn for grain (**CG**), and soybeans (**SBM**) were grown with ^{15}N-labeled fertilizer to enrich these 4 commonly used dairy feeds. The protocol for labeling the feeds was described in detail by Powell et al. (2017). Briefly, crops labeled AS, CS, CG, and SBM were grown by applying ^{15}N-labeled fertilizer to the fields; in adjacent fields, the unlabeled crops were grown with unlabeled fertilizer. The chemical composition and ^{15}N atom percent (**AP**) of unlabeled (i.e., natural abundance of ^{15}N) and ^{15}N-labeled feed ingredients are reported in Barros et al. (2017). The experimental diets included a mineral premix plus the 4 major feed ingredients (AS, CS, CG, and SBM) in the same proportions across treatments. In each treatment, only 1 of the feeds was ^{15}N-labeled (Table 1).

Data Collection

The University of Wisconsin–Madison (Madison, WI) Institutional Animal Care and Use Committee approved all study procedures. Cows, diets, experimental design, and laboratory analyses were detailed in Barros et al. (2017). Briefly, dietary treatments were fed to 12 lactating Holstein cows (means ± SD; 264 ± 18 DIM) for 4 d and urine, feces, and milk were collected dur-

Table 1. Description of treatment diets and animal performance[1]

Item	AS	CS	CG	SBM
Diet ingredient (g DM/kg DM)				
Alfalfa silage	311	312	335	334
Corn silage	319	337	320	321
Dry corn grain	214	203	194	190
Soybean meal	130	126	134	131
Vitamin and mineral mix	26	22	17	24
Nutrient composition (g DM/kg DM)				
Crude protein	175	174	182	177
Rumen-degradable protein[2]	121	120	127	125
Rumen-undegradable protein[2]	54	54	55	54
aNDFom	260	262	262	258
^{15}N, APE (%)	0.251	0.206	0.189	0.247
Animal performance[3]				
FPCM, kg/d	26.5	26.6	24.7	28.9
N Intake, g/d	645	644	636	628
Milk N, g/d	152	144	137	158
Urinary N, g/d	249	242	235	236
Urinary urea N, g/d	191	177	180	178
Fecal N, g/d	164	173	167	161

[1]Detailed description of diet and animal performance can be found in Barros et al. (2017). Diets are identified by their ^{15}N-labeled ingredient: AS = alfalfa silage; CS = corn silage; CG = corn grain; and SBM = soybean meal.

[2]NRC (2001) predicted value.

[3]All *P*-values >0.70; FPCM = fat- and protein-corrected milk, calculated as milk production (kg/d) × [0.01226 × fat (g/kg) + 0.00776 × protein (g/kg) + 0.2534].

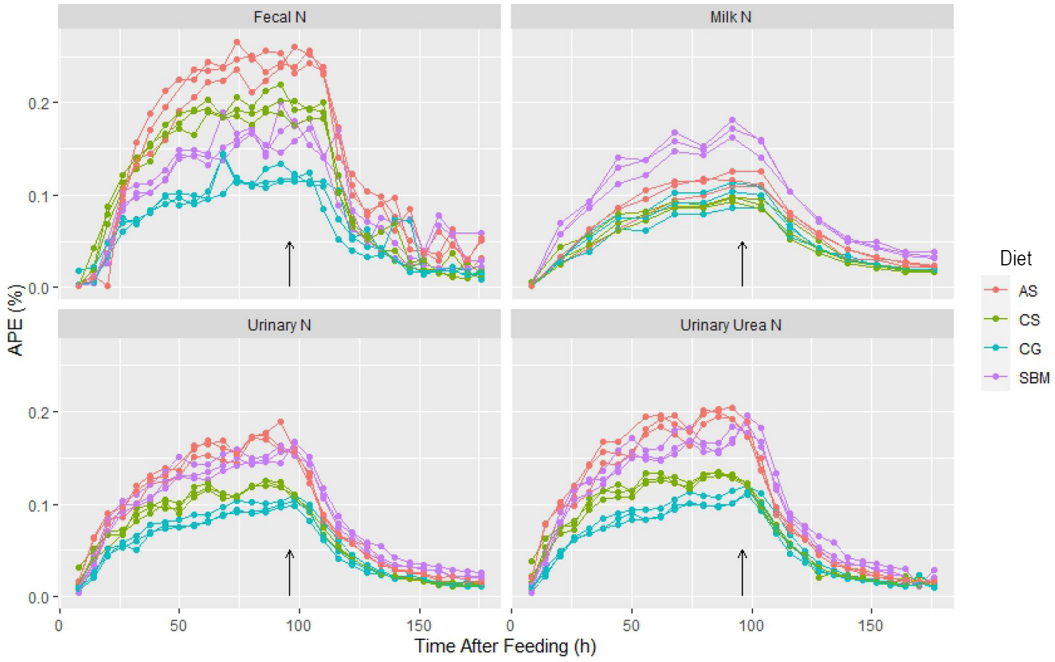

Figure 1. Atom percent excess (APE) for fecal N, milk N, urinary N, and urinary urea N plotted against time starting at initiation of feeding ^{15}N-labeled dietary treatments (AS = alfalfa silage, CS = corn silage, CG = corn grain, and SBM = soybean meal). Each point represents 1 of 3 individual cow observations per time point, with lines connecting observations within cow. Arrows indicate time of last labeled feeding.

ing and after feeding of the ^{15}N-enriched diets. Cows were fed a pretreatment (unlabeled) TMR once daily (at 0800) for 11 d (see Table 2 in Barros et al., 2017) for ingredient and chemical composition of the diets). Before feeding on d 12, cows were blocked by milk yield and randomly assigned within block to 1 of 4 dietary treatments, which were constructed by replacing unlabeled AS, CS, CG and SBM from the pretreatment diet with its analogous ^{15}N-labeled feed. After 4 d of feeding the ^{15}N-enriched TMR, cows were returned to the unlabeled TMR during d 16 to 19. The amount of TMR offered was adjusted daily to ensure 5% of refusals. Cows were milked twice daily (0400 and 1600 h). From d 11 to 19, daily milk production was recorded and milk samples were collected at each milking. Procedures for milk analysis can be found in Barros et al. (2017). Urine and fecal sampling were performed every 6 h (at 0400, 1000, 1600, and 2200 h) from d 12 to 19 and analyzed for total N and ^{15}N. Urinary urea-^{15}N was isolated using an adaptation of the procedure published by Brooks et al. (1989), where the filter traps were placed in a tin analyzer capsule. The tin analyzer cups were folded and analyzed for N and ^{15}N isotope using a Costech 4010 elemental analyzer (Costech Analytical Technologies Inc., Valencia, CA) interfaced to a Thermo-Finnigan Delta-Plus Advantage isotope ratio mass spectrometer (Thermo-Electron GmbH, Bremen, Germany).

Model Development

Barros et al. (2017) presented the AP in unlabeled (natural abundance) and labeled feeds. Atom percent is the ratio of ^{15}N atoms to the total N atoms, calculated as $100 \times [^{15}N/(^{15}N + ^{14}N)]$. Above natural abundance (**ANA**, mg) was calculated as the mass of ^{15}N that exceeded the natural ^{15}N abundance. Atom percent excess (**APE**, %) was calculated by subtracting the natural abundance AP from the experimental AP. Plots of total exit pool ^{15}N ANA versus time (not shown) revealed large variations of ANA by time of day due to diurnal variations in volume of secretion and excretion. Thus, APE was chosen as the measurement of interest for subsequent model fitting because it represents the change in ^{15}N enrichment rather than excretion (Figure 1).

Statistical analyses were conducted in R statistical software v. 4.2.1 (R Foundation for Statistical Computing). Models were fit using the lmer packages for the linear models and the nlme package for the nonlinear models (Pinheiro et al., 2017). The data included observations from 2 phases of change in ^{15}N APE (%): ^{15}N enrichment during the ^{15}N feeding phase from $t = 0$ to $t = 96$ h (rising curve) and a decrease in ^{15}N enrichment from $t = 96$ to $t = 176$ (decay curve) when unlabeled diets were fed. We investigated several modeling approaches that ranged from linear regression of transformed observations to a

compartmental model to predict the measured outcomes simultaneously. Simple linear regression did not provide a good fit to the data, and we were unable to achieve convergence of parameter estimates using a compartmental model. For this reason, we chose to fit nonlinear exponential models to APE observations in FN, UN, urinary urea N (**UUN**), nonurea urinary N (**NUUN**), and MN separately and for each experimental phases.

Single-pool exponential models were fit to the rising (**M1**) and decaying (**M2**) curves separately, followed by a piecewise exponential model fit to the entire data set (**M3**). Although the diets provided during the decay phase included unlabeled feeds that were consistent across treatments, we assumed that some N from labeled feed ingredients fed during the enrichment phase remained in the animal (digestive and other metabolically active organs). Therefore, we chose to include feed-specific parameters in M2. Details of the structure of these models are provided in Table 2 and Appendix 1. In addition, we attempted to fit 2-pool exponential models but were unable to achieve convergence of parameter estimates. The stochastic model was built with increasing complexity to improve fit as described by Strathe et al. (2010) and in Appendix 2. Briefly, the baseline error structure with independent and identically distributed errors and no random effects was adapted to represent the experimental design by including an additive random effect for the animal to each parameter. A first-order autoregressive (**AR-1**) covariance structure was then added to the model to account for correlations associated with repeated measures. Finally, a weighted AR-1 covariance structure was developed to give additional weight to observations at the beginning (M1) and end (M2) of the trial to accommodate APE values very close to zero during those periods. Plots of observed versus predicted, standardized residuals versus time, and standardized residuals versus predicted values, as well as quantile-quantile plots of residuals, were used to assess model fit and the assumption of normality of the error structure.

Model Evaluation and Inference

The need to include treatment-specific parameters was determined with an *F*-test of the full model against a reduced model with 1 parameter for all treatments. Additionally, we tested a model allowing different first-order rate constants for enrichment and decay, respectively, versus a model with a single first-order rate constant describing both phases. Multiple comparison tests of parameter differences among treatments (H_0: $\theta_i = \theta_{i'}$ vs. H_1: $\theta_i \neq \theta_{i'}$ [$\theta_i = k_i$, or L_{1i}], where k refers to the first-order rate constant, H_0 is the null hypothesis and H_1 is the alternative hypothesis, *i* indicates the dietary treatments, and L_1 indicates the lag time from the start of the modeled period to the start of the change in enrichment) were performed using the multcomp package (Hothorn et al., 2008). Model evaluation was conducted using the root mean square error (**RMSE**) and decomposition of its error to determine the proportion of error due to random dispersion (**ED**; Bibby and Toutenburg, 1977). Results are given in Table 3.

To enable comparisons among treatments, estimates of asymptotic APE in the exit pools ($\mathbf{A}_i$) were standardized based on total ^{15}N intake for the treatment. Two methods to test for variable N partitioning among treatments were developed and applied to estimates from M1 and M3 only. Estimates from M2 were omitted from inferential analysis of the asymptotic APE because the

Table 2. Descriptions of models for fecal, urinary, and milk ^{15}N atom percent excess (*APE*, %) data collected on dietary treatment *i* (*i* = 1 to 4) when consumed by cow *j* (*j* = 1 to 12) during the first 96 h of sampling (enrichment phase) and the subsequent 80 h of sampling (decay phase) after initiation of labeled feeding

Model	Description	Form[1]	Data
M1	Single exponential model of rising curve	$APE_{ij} = \begin{cases} 0 & t_j < L_{1i} \\ A_i - A_i e^{-k_i(t_j - L_{1i})} & t_j \geq L_{1i} \end{cases}$	Enrichment phase (time equal to 0 to 96 h after labeled feeding)
M2	Single exponential model of decaying curve	$APE_{ij} = \begin{cases} A_i & t_j < L_{1i} \\ A_i e^{-k_i(t_j - L_{1i})} & t_j \geq L_{1i} \end{cases}$	Decay phase (time equal to 0 to 80 h after cessation of labeled feeding)
M3	Piecewise exponential model	$APE_{ij} = \begin{cases} 0 & t_j < L_{1i} \\ A_i - A_i e^{-k_i(t_j - L_{1i})} & L_{1i} < t_j < L_{1i} + L_2 \\ \hat{A}_{(t)i} e^{-k_i(t_j - (L_{1i} + L_2))} & L_{1i} + L_2 < t_j \end{cases}$	Both enrichment and decay phases (time equal to 0 to 176 h after labeled feeding)

[1]A_i is estimated maximum APE of exit pools from a cow fed diet *i*; $\hat{A}_{(t)i}$ is the estimated APE of exit pools from a cow fed diet *i* at the time point t = $L_1 + L_2$; k_i is fractional rate of APE accumulation or decay for the *i*th diet; L_{1i} is the lag from time t = 0 to the time when APE begins to increase in exit pools for the *j*th diet; L_{2i} is the lag from time t = L_{1i} to t = ($L_{1i} + L_{2i}$) when APE of the exit pools from the *i*th diet begins to decay from the maximum APE during the experimental period.

Table 3. Root mean square prediction error (RMSE, % of mean observed value) and percent of error due to randomness (ED) for models M1, M2, and M3, predicting ^{15}N APE in fecal (FN), urinary (UN), urinary urea (UUN), and milk nitrogen (MN)

		FN		UN		UUN		MN	
Model	Model	RMSE	ED	RMSE	ED	RMSE	ED	RMSE	ED
Exponential rise	M1	7.55	99.7	6.24	99.5	6.15	99.2	6.04	99.8
Exponential decay	M2	21.0	95.7	11.4	93.1	14.4	95.1	10.6	96.1
Piecewise	M3	15.3	95.9	10.4	89.0	10.5	98.3	11.2	98.3

model form implies the asymptotic APE was reached during the experimental period, which is not certain. The first method used the change in APE (**ΔAPE**) from dietary intake (**APE$_{\mathbf{In}i}$**) to the exit pool using the model predicted asymptotic APE of the exit pool $\left(\hat{A}_i\right)$ as defined in Equation 1:

$$\Delta\text{APE}_i = \hat{A}_i - \text{APE}_{\text{In}i}. \quad [1]$$

For a given labeled feed, if there is no selective partitioning of N among exit pools, the change in APE from diet to exit is expected to be zero. Therefore, we tested whether $\text{APE}_{\text{In}} - \Delta\text{APE}_i$ differed significantly from zero. Additionally, we tested pairwise differences in feeds (i vs. i') in the extent of selective partitioning among exit pools using the following hypotheses:

$$H_0: \Delta\text{APE}_i = \Delta\text{APE}_{i'};$$

$$H_1: \Delta\text{APE}_i \neq \Delta\text{APE}_{i'}. \quad [2]$$

This was tested using the following t-distributed test statistic,

$$t_{ii'} = \frac{\Delta\text{APE}_i - \Delta\text{APE}_{i'}}{\sqrt{\frac{\text{SD}^2_{\text{prop}i}}{4} + \frac{\text{SD}^2_{\text{prop}i'}}{4}}}, \quad [3]$$

where $\text{SD}_{\text{prop}i}$ is the SD computed by propagating error in the measured SD of the $\text{APE}_{\text{In}i}$ and the model-estimated SD of A_i for i = 1, …, 4 for the 4 dietary treatments. Results are presented in Table 4.

Table 4. Change in ^{15}N enrichment from diet[1] to the predicted asymptotic enrichment in exit pools

			ΔAPE[2]			
Model	Model[3]	Exit pool[4]	AS	CS	CG	SBM
Exponential	M1	FN	-2.85×10^{-3}[a]	-5.36×10^{-3}[a]	−0.0659[ab]	−0.0783[b]
			(0.0410)	(0.0412)	(0.0464)	(0.0439)
Rise		UN	−0.0709†	−0.0832†	−0.0484†	−0.0906*
			(0.0342)	(0.0325)	(0.0392)	(0.0303)
		UUN	−0.0476	−0.0730†	−0.0799†	−0.0743†
			(0.0332)	(0.0323)	(0.0385)	(0.0304)
		MN	−0.114†	−0.0997†	−0.0650†	−0.0650†
			(0.0483)	(0.0421)	(0.0515)	(0.0367)
Piecewise	M3	FN	3.38×10^{-3}[a]	-8.94×10^{-3}[a]	−0.0652[b]	−0.0666[b]
			(0.0338)	(0.0324)	(0.0369)	(0.0371)
Exponential		UN	−0.0842*	−0.0864*	−0.0883*	−0.0855*
			(0.0280)	(0.0289)	(0.0303)	(0.0287)
		UUN	−0.0609	−0.0739†	−0.0798†	−0.0659
			(0.0326)	(0.0329)	(0.0335)	(0.0376)
		MN	−0.122*[a]	−0.101†[ab]	−0.0825†[ab]	−0.0621[b]
			(0.0375)	(0.0374)	(0.0374)	(0.0332)

[a,b]Separation of ΔAPE among treatment means for each exit pool; means within a row that do not share a common letter superscript are different ($P < 0.10$).

[1]Dietary treatments: AS = ^{15}N-labeled alfalfa silage; CS = ^{15}N-labeled corn silage; CG = ^{15}N-labeled corn grain; SBM = ^{15}N-labeled soybean meal.

[2]ΔAPE = Predicted asymptotic APE (atom percent excess) in the exit pools − dietary treatment APE. Asymptotic APE predicted from models fit to the enrichment phase only (M1, 0 to 96 h after initiation of labeled feeding) and to the entire experimental phase (M3, 0 to 176 h after initiation of labeled feeding). SE of estimate provided in parentheses.

[3]Models represent the enrichment phase (M1) and both enrichment and decay phases (M3).

[4]FN = fecal N; UN = urine N; UUN = urinary urea N; MN = milk N.

*,†ΔAPE different from 0, where * signifies $P < 0.05$ and † signifies $P < 0.10$.

The second method, with results presented in Table 5, compared the ratios of the estimates for the asymptotic APE from M1 and M3 $\left(\hat{A}_i\right)$ in FN (R_1), UN (R_2), and UUN (R_3) relative to MN for each feed ingredient (i = 1 to 4). A ratio of 1.0 indicates equal partitioning of intake N to FN or UN relative to MN, whereas ratios greater or less than 1.0 indicate more or less N partitioned to urine or feces relative to milk. These ratios are defined as follows:

$$R_{1i} = \frac{\hat{A}_{FNi}}{\hat{A}_{MNi}},$$

$$R_{2i} = \frac{\hat{A}_{UNi}}{\hat{A}_{MNi}},$$

$$R_{3i} = \frac{\hat{A}_{UUNi}}{\hat{A}_{MNi}}. \quad [4]$$

The test statistic for assessing differences between treatments the difference in the ratios of the estimates for FN/MN, UN/MN, and UUN/MN between treatments divided by the square root of the sum of the APE ratio standard errors. The APE ratio SD were computed by propagation (SD_{prop}):

$$t_{ii'} = \frac{R_{1i} - R_{1i'}}{\sqrt{\frac{SD^2_{propi}}{4} + \frac{SD^2_{propi'}}{4}}}. \quad [5]$$

To enable comparison with nutrient requirement models, we estimated the proportion of exit N from each feed excreted (FN, UN) or secreted (MN) using Equation 6 and Equation 7 and the underlying assumption that deviation of the exit pool ^{15}N AP is a result of excretion of N originating from the labeled feed, as follows:

$$prop_i = \frac{\hat{A}_i}{APE_{Feed_i}}. \quad [6]$$

In Equation 6, APE_{Feed_i} represents the APE of the labeled feed. Details on the derivation of Equation 6 are provided in Appendix 3. For each exit pool, $prop_i$ were summed for across all 4 feeds and subtracted from unity to estimate the proportion of N from endogenous sources rather than feed inputs, similar to Leterme et al. (2000). To allow for comparison with nutritional models (see the following section, "Adaptation of Existing Nutritional Models"), we changed the basis of the proportion to correct for incomplete fractional recovery of labeled N. Within each exit pool, the proportion of labeled N from feed i in the total recovered labeled N was calculated as

$$prop\_of\_recovered_i = \frac{prop_i}{\sum_{i=1}^{4}(prop_i)}. \quad [7]$$

Table 5. Asymptotic ^{15}N enrichment in fecal, urine, or urinary urea N relative to ^{15}N enrichment in milk N, for each dietary treatment[1]

			Dietary treatment			
Model	Model[2]	Ratio[3]	AS	CS	CG	SBM
Exponential	M1	FN/MN	1.81*[a] (0.0991)	1.88*[a] (0.105)	0.993[b] (0.0822)	0.926[b] (0.0381)
Rise	M2	UN/MN	1.31*[a] (0.0715)	1.15†[b] (0.0648)	0.840†[c] (0.0654)	0.859*[c] (0.0246)
		UUN/MN	1.48*[a] (0.0792)	1.25*[b] (0.0689)	0.880[c] (0.0668)	0.949[c] (0.0263)
Piecewise	M3	FN/MN	1.97*[a] (0.0702)	1.87*[a] (0.0801)	1.16†[b] (0.0597)	0.976[c] (0.0316)
Exponential		UN/MN	1.30*[a] (0.0463)	1.14†[b] (0.0510)	0.945[c] (0.0453)	0.873*[d] (0.0241)
		UUN/MN	1.48*[a] (0.0545)	1.26*[b] (0.0586)	1.02[c] (0.0512)	0.979[c] (0.0287)

[a–d]Separation of treatment means for each ratio; means within a row that do not share a common superscript are different ($P < 0.05$) based on an independent t-test with unequal variances, using error propagation to estimate variances for each ratio.

[1]Dietary treatment: AS = ^{15}N-labeled alfalfa silage; CS = ^{15}N-labeled corn silage; CG = ^{15}N-labeled corn grain; SBM = ^{15}N-labeled soybean meal.

[2]Models represent the enrichment phase (M1), decay phase (M2), and both enrichment and decay phases (M3).

[3]FN = fecal N; UN = urine N; UUN = urinary urea N; MN = milk N. SE of the estimates provided in parentheses.

*,†Ratios different from 1, where * signifies $P < 0.05$ and † signifies $P < 0.10$.

Adaptation of Existing Nutritional Models

Proportions of excreted N traced to each feed as estimated by application of model results in Equation 7 were compared with estimates based on NRC (2001) and NASEM (2021) models, using the measured milk CP, DMI, body weight, and feed composition from our experiment as inputs. To generate estimates of N excretion from individual feeds comparable to those of M3, both NRC (2001) and NASEM (2021) models had to be extended with certain assumptions. Both models required the assumption that protein fractions were sourced from feeds in proportion to diet composition. Additional assumptions are detailed in Appendix 4.

RESULTS AND DISCUSSION

In the preliminary report of this study, Barros et al. (2017) presented data on cow performance and N partitioning (g/d and g/N intake) and established that the isotope labeling that defined the treatment diets did not affect milk production or N use efficiency.

Model Selection and Fit

Nested model comparisons indicated no improvement in fit when allowing first-order rate constants specific to enrichment and decay phases; therefore, a single first-order rate constant was used. The AR-1 covariance structure with random effects for cow showed a significant improvement in model fit based on the *F*-test ($P < 0.05$), reduced Akaike information criterion and Bayesian information criterion, and reduced patterns in the residuals over a simple covariance structure or 1 with only random effects for cow. When residuals were weighted by the inverse of the observed mean at each time point, the residual patterns plotted against time and fitted values showed substantial improvement, so the full covariance structure with weighted residuals was used for all models.

Table 3 shows the decomposition of error for the exponential rise (M1), decay (M2), and piecewise (M3) models for each exit pool. The RMSE was the lowest for M1 prediction of MN 6.04% of the observed mean) and the highest for M2 prediction of FN (21.0% of the observed mean). For each model, the RMSE was substantially greater for FN than for UN, MN, or UUN. Furthermore, for all pools of N, RMSE were the lowest for M1, the greatest for M2, and intermediate for M3, with the exception of MN, in which case the RMSE of M3 was close to but slightly higher than that of M2. Differences in prediction error estimates are, in part, a result of the difference in observed data used in each model. The greater prediction error in the decaying curve (M2) than the enrichment phase (M1) could be an indication that a single-pool model is less appropriate for M2 than M1 and be taken as evidence for a need for a 2-pool model to better describe dynamics of N digestion and metabolism, although we were not able to achieve convergence for this model. Decomposition of the error indicated the models had little bias, with greater than 90% of the error due to random dispersion in all but 1 model (Table 3). Overall, these results indicated that the chosen model structures fit the data well.

Nitrogen Partitioning

Table 4 shows ΔAPE, the differences between A_i and intake APE provided by M1 (the enrichment phase) and M3 (enrichment and decay phases), the first method used to test for differential partitioning of feed N to exit pools among feed. Estimates of asymptotic ^{15}N APE in feces were not different ($P > 0.10$) than dietary APE for any of the feeds in neither M1 nor M3. However, the ΔAPE for both concentrates were more negative than those of both forages in M3, and that of SBM was more negative than both forages in M1. The absence of change in ^{15}N enrichment from diet to feces indicates that the proportional contribution of the labeled feed N to total FN was the same as the feed contribution to total dietary N. However, the greater negative dietary ΔAPE in concentrate feeds compared with forages suggests that overall N in concentrate feeds were partitioned away from feces to a greater extent than forage N. These results may reflect a greater true digestibility of N in concentrate than forage, a greater recycling of labeled N (urea N, endogenous N, or both) from the body to the gastrointestinal tract of forage N than concentrate N, or a combination of both. Although FN and ^{15}N were not decomposed further to determine the proportions attributed to feed, microbial, and endogenous N as in Ouellet et al. (2002), our results indicated that the contributions of the feeds to each of the FN fractions, to recycled N, or both, varied substantially between the forages and concentrates used in this study.

Unlike FN, estimates of UN APE were significantly less ($P < 0.10$ or $P < 0.05$) than dietary APE for all feeds in both M1 and M3 models, with values for ΔAPE remarkably consistent and ranging from −0.0484 to −0.0906 between models and among feeds.

Regarding MN ΔAPE, both models indicated a significant reduction in asymptotic ^{15}N APE for MN compared with dietary N for AS, CS, and CG, whereas only M1 indicated a significant ($P < 0.10$) reduction for SBM. Although the test comparing ΔAPE for SBM with feed APE was not significant ($P = 0.17$), the estimates of ΔAPE_i from M3 were significantly different ($P < 0.10$) among treatments. The negative MN ΔAPE was twice as large for AS than for SBM (−0.122 vs. −0.0621 re-

Table 6. Comparison of piecewise nonlinear model (M3 of this study) with NRC (2001) and NASEM (2021) predicted proportion of N from individual feeds in feces, urine, and milk (feed excretion N, g/total recovered excretion N, g)[1]

Body pool	Model	Exit pool proportion of N from feeds[3]	Dietary treatment[2]			
			AS	CS	CG	SBM
Feces	M3	0.822	0.430	0.174	0.0741	0.321
	NRC		0.446	0.196	0.0627	0.296
	NASEM		0.392	0.167	0.0961	0.345
Urine	M3	0.605	0.383	0.144	0.0820	0.391
	NRC		0.398	0.114	0.0757	0.412
	NASEM		0.390	0.154	0.0773	0.379
Milk	M3	0.579	0.309	0.132	0.0907	0.468
	NRC		0.249	0.169	0.144	0.438
	NASEM		0.344	0.149	0.0920	0.415

[1]NRC (2001) and NASEM (2021) models were extended with assumptions detailed in the text and in Appendix 4.
[2]Dietary treatment: AS = ^{15}N-labeled alfalfa silage; CS = ^{15}N-labeled corn silage; CG = ^{15}N-labeled corn grain; SBM = ^{15}N-labeled soybean meal.
[3]For each exit pool, the proportion of total ^{15}N intake above natural abundance in that pool from each feed was summed across all 4 feeds to achieve an estimate of the total contribution of feed N to each exit pool.

spectively; Table 4). These results suggest that SBM feed N is partitioned toward milk to a greater extent and AS feed N is partitioned toward milk to a lesser extent, whereas the feed N partitioning to MN from CS and CG appear to be intermediate between the 2 legume feeds. Conversely in both M1 and M3, the ΔAPE for UN and UUN were numerically more negative for SBM than AS. The change in the direction of the relationship of ΔAPE_i between MN and the urinary routes of excretion for AS and SBM could indicate that the absorbed N from SBM is partitioned more toward milk instead of the urinary route of excretion in comparison to the absorbed N from AS. A likely factor in this observation is the expected differences in rumen degradability and subsequent absorption of ammonia across the rumen wall.

The ratios of the A_i in FN, UN, and UUN to MN are shown in Table 5, and outcomes align with the analysis of ΔAPE_i in Table 4. Specifically, the ratios of asymptotic enrichment in FN/MN and UN/MN for concentrate feeds were significantly less than the enrichment ratio for forage feeds. Whereas forage FN/MN and UN/MN enrichment ratios exceeded 1.0, indicating more N was partitioned to manure compared with milk ($P < 0.10$ for the CS UN/MN ratio; $P < 0.05$ otherwise), the concentrate UN/MN and FN/MN ratios were either not different than 1 (indicating that a similar fraction of the feed N was partitioned to milk compared with manure) or significantly less than 1 (indicating a greater fraction of the feed N was partitioned to milk compared with manure). One exception to this pattern was the ratio of FN/MN for CG estimated by M3 which was larger than 1 (1.16, $P = 0.083$). The comparison of the ratios of FN/MN and UN/MN among feeds estimated by nonlinear models in the present study is in line with the ratios of values measured on the fourth day of feeding ^{15}N-enriched diets (Barros et al., 2017). Together, our results indicate that in forage feeds, a greater fraction of feed N is partitioned to both feces and urine than milk in comparison to concentrate feeds.

Comparison of N Partitioning with Nutritional Models

Table 6 shows the proportion of labeled N from each feed in the total recovered labeled N from all exit pools. As implied by M3, N from feed intake made up 82.2% of the total FN during the experiment (95% CI: 80.5%–83.9%). The remaining FN (17.8%) not attributed to intake represents endogenous N. This M3 estimate is in line with measured endogenous N (17% of FN) in the 200-h ^{15}N infusion trial by Ouellet et al. (2002). The proportion of endogenous N was greater in UN (39.5%) and MN (42.1%) than FN. Researchers have reported the large contribution of whole-body protein turnover to total protein synthesis, yet due to the high turnover rates and low net gain, a much lower fraction of total protein synthesis from gastrointestinal tract is considered net gain (milk protein secretion or body tissue gain) when compared with the mammary gland and peripheral tissues (Bequette et al., 1996; Lobley, 2003). Further, the cows in this trial were in late lactation (DIM = 264); thus, the high contribution of body N to MN and UN is likely a result of typical protein turnover rather than the net mobilization of body reserves.

Table 6 also compares the results of M3 with the N partitioning implied by extending the NRC (2001) and NASEM (2021) nutritional models, where we see that the M3 estimates are generally consistent with those of the NRC and National Academies of Science, Engineering,

and Medicine (**NASEM**) models. The M3 estimates for the proportion of the recovered FN from each feed M3 were always intermediate to the NRC and NASEM estimates. More specifically, NRC predicts a greater proportion of FN originating from the forage feeds and a lesser proportion of FN originating from the concentrate feeds than the estimates provided by M3. The comparison of NASEM estimates with M3 is reversed: lower predicted proportions of FN from forages and higher proportions of FN from concentrates for NASEM in comparison to M3. The different pattern in the comparison of the estimates of FN from forage and concentrate feeds from M3 and the nutrient requirement models can be explained by the changes to the parameter estimates for the fraction of indigestible N between the models. The indigestible N fractions of AS and CS in the NASEM (2021) feed library are 9% and 16% of total N, respectively, AND those from the NRC are 9.9% and 18.5%, respectively. Similarly, the intestinal digestibilities for CG and SBM in the NASEM feed library are less than those in the NRC.

The 3 models predicted similar proportions of N in urine from each feed, except that NRC predicted a smaller proportion of UN from CS and greater proportion of UN from SBM. For milk, NRC predicted a lesser and NASEM predicted a higher proportion of MN from AS than M3. The NRC model also estimated a greater proportion of MN from CS and CG than M3 and NASEM. The proportion of MN originating from SBM estimated by M3 is greater than both NRC and NASEM models. The NASEM estimates were numerically closer to M3 than NRC for most comparisons of UN and MN suggesting improved feed-level performance for predicting UN and MN with the updated model, especially for CS and CG. The greater proportion of N from AS in MN with M3 and NASEM than with NRC may relate to NRC predictions of microbial crude protein (**MCP**), which were lesser than NASEM. Additionally, the NRC model allocated protein supply to body pools on an MP rather than AA basis, as represented in NASEM and physiologically (as modeled by M3). This may explain NRC's overprediction of MN from CG and underprediction of MN from AS relative to M3. NASEM (2021) reported similar AA composition between microbial true protein and milk true protein and, in our study, a large fraction of diet RDP was supplied by AS.

Nitrogen Kinetics

Estimates for both lag ($\mathbf{L}_i$, h) and rate of turnover (enrichment or decay; $\boldsymbol{k}_i$, 1/h) are related to the rate of feed N excretion in FN, UN, UUN, and MN and are illustrated in Figures 2, 3, and 4 (numerical values presented in Appendix 5). For feces, larger FN-L_{CS} indicated significantly longer lag time than FN-L_{SBM} in both the exponential decay (M2) and piecewise (M3) models. However, for the exponential rise model (M1) that exclusively used the enrichment data, FN-L_{AS} was significantly longer than all other feed lag times (Figure 2). The discrepancy in the relative order of lag time estimates between the rising and decaying curve estimates could reflect the varying kinetics in the fractions that make up FN and the different contributions of each feed to those fractions. Elucidation of this relationship would require that the pools of FN and their enrichment be investigated instead of total FN alone.

Estimates for the rate of ^{15}N change in feces (FN-k_i) were numerically greater for the forages than the concentrate feeds for all models, although significant differences were only detected for comparison of k_{CS} with the rates for concentrate feeds predicted by M2 and M3 (Figure 3). The constant, k_i, represents the rate at which the labeled feed is replacing N from the unlabeled feed in that pool, or the rate of turnover. Assuming a steady state, the rate of turnover of undigested feed N in FN is equal to the rate of passage divided by the indigestible intake N pool size. One would expect the indigestible N pool size as a fraction of total N to be larger for grain forages (i.e., CS) than legume forages (i.e., AS) and concentrate feeds and expect the rate of passage to be correspondingly lower as a result of a longer retention time and a slower rate of undigested N turnover, which is contrary to M2 and M3 predictions for the CS rate of turnover. However, indigestible N is only one source of FN, and as with the lag estimates, aggregation of the FN components masks what is likely a varying rate of turnover for different FN component between feeds.

Understanding the rate of turnover of the microbial N pool from each feed is more challenging. A substantial amount of recycling (between 40% and 70% of the pool) occurs within the microbial N pool due to a combination of lysing and predation by protozoa (Dijkstra et al., 1998). Thus, the microbial N pool has a slower rate of turnover (longer retention time) than that of feed N pools. Within the microbial N pool, the rate of turnover of a feed's contribution to the microbial N pool depends on the rate of microbial synthesis from that pool, the total rate of turnover of microbial N, and the rate of passage of microbial N. In this study, the rate of passage of microbial N and microbial N turnover rates are not expected to vary because the diet composition is the same across treatments, but the rate of microbial protein synthesis and N turnover from each feed will vary. As a proportion of CP, the forage feeds in our study have more soluble and degradable protein than the concentrate feeds, from which microbial protein is synthesized at a faster rate than the remaining RDP (NRC, 2001). Thus, the faster FN-k_i estimates for CS could reflect a faster rate of turnover of its N in the microbial N pool in comparison to

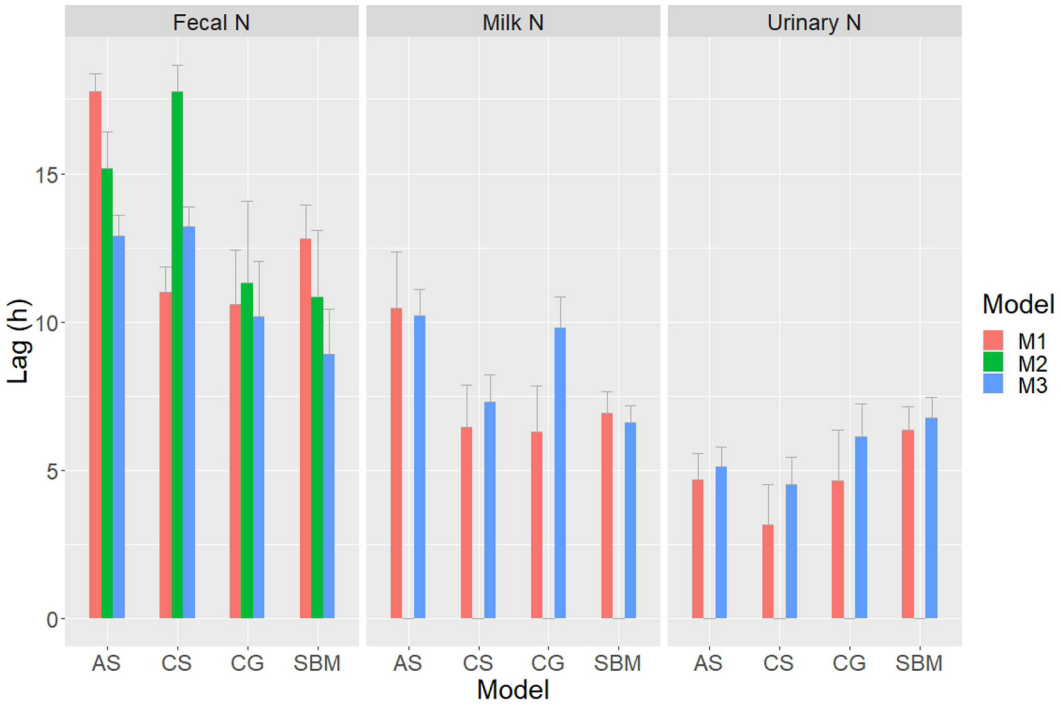

Figure 2. Comparison of lag time parameter estimates (Lag) from 3 different models (M1 = enrichment phase, M2 = decay phase, and M3 = both enrichment and decay phases) representing the delay in N^{15} appearance in fecal N, urinary N, and milk N from feeding ^{15}N-labeled dietary treatments (AS = alfalfa silage, CS = corn silage, CG = corn grain, and SBM = soybean meal). M2 lag parameters were fixed to zero for milk N and urinary N based on model fit. Error bars indicate the SE of the parameter estimates.

the other feeds. Thus, these results highlight the need for further research to separate the different FN fractions to further elucidate the digestion kinetics of feed N.

Unsurprisingly, kinetic parameter relationships between feeds were the same for both UN and UUN because UUN made up over 70% of total UN (Barros et al., 2017), although more significant differences were detected between estimates for UUN lag parameters between feeds (Figure 4, Appendix 5). The estimates of the lag time associated with the appearance of N in cows fed SBM (L_{SBM}) for both UN and UUN was longer than that of the other feeds while the lag times for N from CS (L_{CS}) were always shorter than those of other feeds (Figure 2). The only statistically significant differences found, however, were in the comparison between the M3 estimates for the forage feeds (UUN-L_{CS} and UUN-L_{AS}) and UUN-L_{SBM} ($P < 0.05$). It is unclear what physiological processes would cause a longer delay in the N excretion from SBM than AS and CS in UUN. Comparisons of the rates of ^{15}N enrichment and decay between feeds in estimates for k_i did not produce any consistent patterns, and the only significant differences detected were between k_{AS} and k_{SBM} for UN and UUN in the model fit to the decaying curve data (M2). The fastest rate of change in UN and UUN (largest k_i estimates) from M2 were predicted for the treatment with labeled AS (Figure 3). Unlike the estimates for the lag time where the numerical differences reflected a similar pattern to the significant differences, the numerical differences between estimates of UN-k_i and UUN-k_i from the other models (M1 and M3) did not follow a similar pattern to the significant differences found in M2. To investigate if there are metabolic factors contributing to the rate of excretion and secretion of UN and MN from specific feed sources, future work should include an assessment of blood AA (**AA-N**) and blood urea N and their enrichment curves.

Comparison of the kinetic parameter estimates between the exit pools mostly agreed with our current knowledge of ruminant digestion and metabolism. All lag estimates (L_i) for UN and MN were smaller than those for FN (Figures 2 and 4, Appendix 5). The shorter lag time for ^{15}N to begin to appear in MN and UN is a result of urea N originating primarily from ammonia N absorbed across the rumen wall rather than milk protein N secretion or other N metabolites found in urine. Some ^{15}N is also expected to end up in NUUN. We estimated NUUN APE as the difference in ^{15}N enrichment in UN and UUN, weighted by urea concentration. We found that NUUN APE was less than 0.1 for all treatments (in comparison to less than 0.2 for UUN; Appendix 6). Nonurea urinary N is made up mostly of N in purine derivatives that are metabolic byproducts of microbial nucleic acids and creatinine N that originate from the breakdown of muscle creatine excreted at a constant rate in proportion to the amount of skeletal

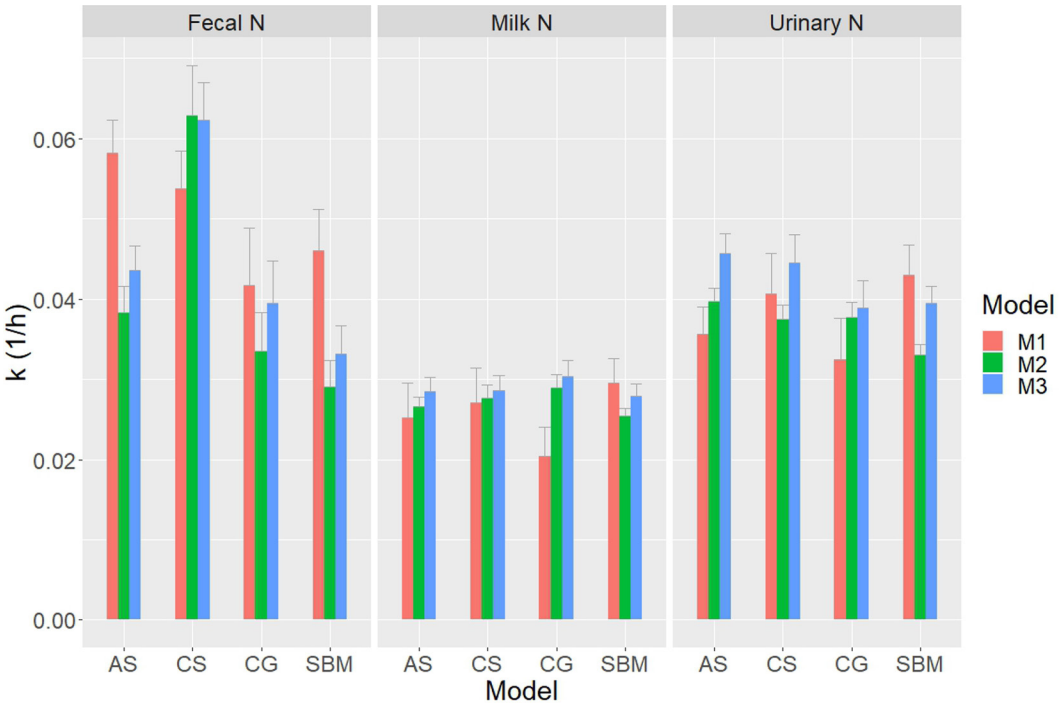

Figure 3. Comparison of rate of enrichment and decay parameter estimates (k) from 3 different models (M1 = enrichment phase, M2 = decay phase, and M3 = both enrichment and decay phases) in fecal N, urinary N, and milk N from feeding ^{15}N-labeled dietary treatments (AS = alfalfa silage, CS = corn silage, CG = corn grain, and SBM = soybean meal). Error bars indicate the SE of the parameter estimates.

muscle tissue. Turnover of microbial N (1–2 d, Dijkstra et al.,1998) and skeletal muscle nitrogen (>200 d, Lobley, 2003) is much slower than blood urea N turnover; thus, the lag time and rate of enrichment for the NUUN pools are likely longer and slower than UUN. Given that total UN is composed of UUN and NUUN, we would hypothesize that the lag time estimates of UN would be the same as those of UUN and the rate of enrichment estimates of UN to be smaller than those of UUN. Our results generally align with this hypothesis, as we see that the estimates for UUN-k_i are consistently numerically higher than those of UN-k_i with the magnitude of the differences between the estimates for k_i ranging between 0.75 and 2.2 SE. The only exception to this relationship was found in the estimates for k_{CG}, by M2 in which the estimate for UN-k_{CG} was less than 0.20 SE above that of UUN-k_{CG}. Although the estimates for UUN-L_i were most often numerically greater than the estimates for UN-L_i within models and feeds, the numerical differences are relatively small (often ~0.5 h or less and always less than 1 SE of any of the estimates).

The MN enrichment rate estimates are also slower than those of UUN, whereas the lag times are on average more than 2 h longer than the estimates for UUN-L_i. The exception to the observed longer lag times when comparing MN-L_i to UUN-L_i are the estimates for MN-L_{SBM}, where the estimate from M1 was similar to that of UUN-L_{SBM} (difference of 0.030 h) and the estimate of MN-L_{SBM} from M3 was 0.710 h longer than that of UUN-L_{SBM}. Unlike UN, MN is mostly composed of true protein N, with a very small fraction coming from urea N. The slower rate of enrichment combined with the smaller proportion of MN originating directly from intake N (Table 6) point to a large fraction of MN being sourced to a greater extent from body tissues. In other words, our data suggested that a substantial proportion of the absorbed AA-N from feed is incorporated into body protein, potentially limiting availability of AA from feed for milk protein synthesis. This illustrates the importance of future research on the slow turnover body N pool(s) models of dairy cattle N metabolism to fully elucidate the long-term N efficiency of diets and feeds.

Limitations and Experimental Methodology

The percentage of N intake recovered through the total collection of milk, urine, and feces ranged from 85 to 88% (Table 1). Although the recovery of N intake was incomplete, this outcome has minimal impact on our results because the analysis and inference are based on measurements of ^{15}N from samples collected throughout the study period. However, it is still likely that circadian variation in the composition of N in milk, urine, and feces (e.g., Gustafsson and Palmquist, 1993),

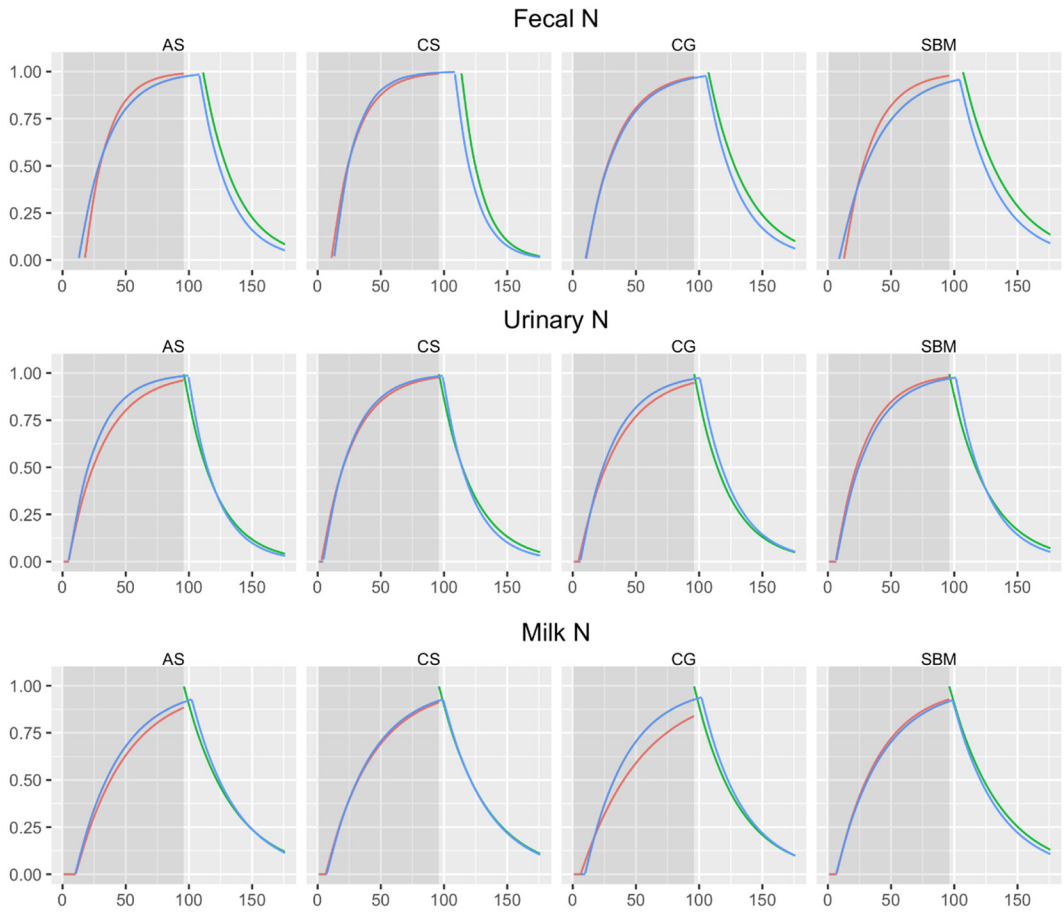

Figure 4. Predicted ^{15}N enrichment in fecal N, urinary N, and milk N using models from 3 different phases (M1 = enrichment phase, M2 = decay phase, and M3 = both enrichment and decay phases) of a stable isotope trial in which 1 of 4 feeds (AS = alfalfa silage, CS = corn silage, CG = corn grain, and SBM = soybean meal) were intrinsically labeled with ^{15}N. Enrichment values are standardized to their means to create a standard scale from 0 to 1.

combined with the incomplete recovery of N, influenced our ability to completely capture the enrichment dynamics.

Model fits and parameter estimates not only revealed limitations of the current data set, but also suggested improvements to experimental design for use of ^{15}N stable isotopes to compare N partitioning and kinetics in different feeds. For example, future studies could sample more body tissues (e.g., plasma and intestinal mucosa as in Ouellet et al., 2002) to enable differentiation between feed and microbial N in FN. This would enable comparisons of each feed's rate of incorporation and total contribution to microbial N production. Similarly, measuring ^{15}N enrichment in urine or plasma purine derivatives or creatinine could facilitate estimation of feed N contribution to microbial and skeletal muscle turnover.

Plots of residuals against time (Figure 5) point to another improvement in experimental design in addition to providing support for the existence of slow turnover pools. The residual plots show a pattern of increasing residual values near the end of the experimental period. This trend toward larger positive residuals at the end of the experimental period indicated that the observed APE values for all exit pools and treatments were increasingly more than the predicted values. Thus, the models are predicting a return to natural abundance (APE = 0) earlier than is suggested by the data. This feature of the data is, again, likely attributable to 1 or more slow N turnover pools of body protein N. Based on fractional rates of protein synthesis and degradation estimated in sheep and cattle, the time course for our experiment would allow extensive protein turnover in splanchnic and mammary tissues but limited turnover in peripheral tissues such as skeletal muscle (Lobley, 2003). In this study, the last sampling was 80 h after the final isotope-containing meal, at the end of which the ^{15}N APE had not returned entirely to baseline (Figure 1). Thus, because this trial was not long enough to substantially or completely label slow turnover pools of body tissue, our estimates of the contribution of endogenous N to each exit pool describe

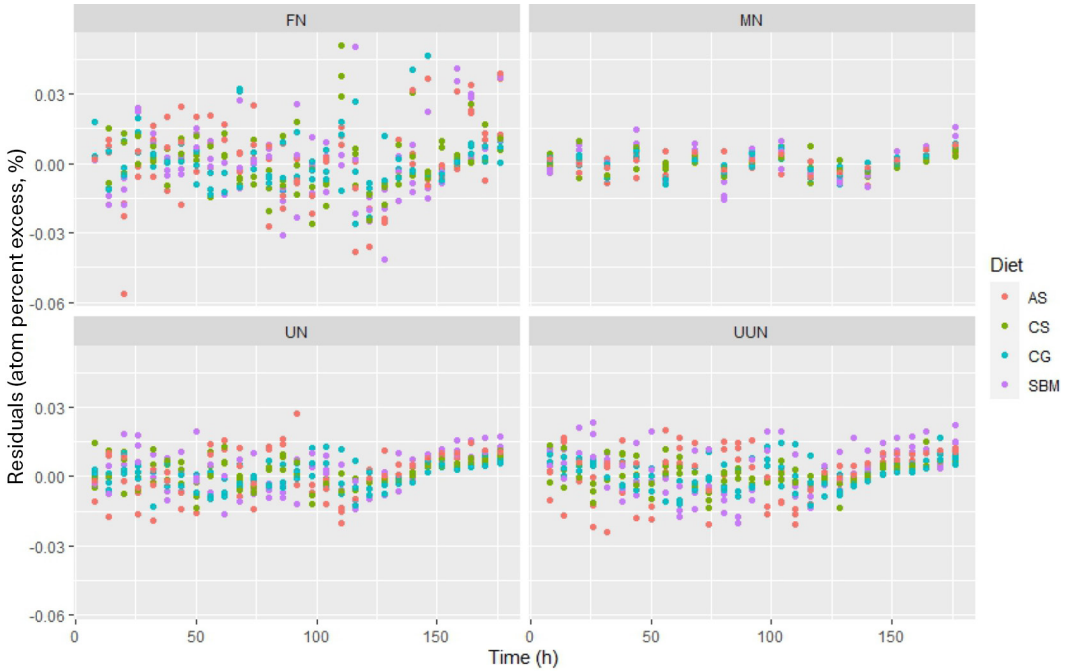

Figure 5. Residuals (atom percent excess, %) from the piecewise model (M3) for fecal N (FN), urine N (UN), milk N (MN), and urinary urea N (UUN) plotted against time (h) from feeding ^{15}N-labeled dietary treatments (AS = alfalfa silage, CS = corn silage, CG = corn grain, and SBM = soybean meal).

the proportions of N originating mainly from pools with protein turnover rates less than 25%/d.

Extending the data collection period during the decay period and more frequent sampling during the early decay period could improve estimation of the kinetics of this pool by providing the statistical power to fit a 2-pool model. Cantalapiedra-Hijar et al. (2020) were able to fit a 2-pool exponential model of ^{15}N decay in UN over a much longer time period (142 d) from steers fed diets enriched in ^{15}N via labeled urea. In their analysis of the suitability of a single or 2 pool model, they found evidence for a change in the rate of decay between d 4 and 7 after cessation of ^{15}N feeding. Thus, we believe we have only or predominantly captured the dynamics of the fast turnover pool, and future work should extend the sampling period at least 7 d after cessation of isotope delivery if study objectives are related to body tissue protein turn over.

Some authors reported that isotopes fractionated differentially to certain body pools based on in vitro (e.g., Wattiaux and Reed, 1995) and in vivo (Cantalapiedra-Hijar et al., 2015) studies of N isotopes at natural abundance, and that dietary characteristics could affect the extent of differential fractionation. Differential fractionation is expected to minimally affect deliberate tracer studies such as our study but may be an important consideration for future studies on natural abundance.

There are also limitations in the form of the models used beyond the restriction to a single-pool model imposed by the data. First, M1 and M2 are only able to use a subset of the data set to inform the parameter estimates because the models describe either an enrichment or decay process. Creation of the piecewise model accommodates the use of the complete data set, which contains more information about the shared kinetic parameters than a data subset.

The exponential model for the decay curve (M2) requires an assumption of when the decay process starts. We chose to start with the sample collected after the first nonlabeled meal was delivered, however, the model was unable to estimate L_i for UN, UUN, and MN under this assumption. This limitation is also avoided in the piecewise model (M3) by defining the cut-off point between the rising and decaying curve as an estimated parameter rather than a predetermined time point.

CONCLUSIONS

Our results suggested that absorbed N from the concentrate feeds (CG and SBM) was incorporated into milk at a higher proportion than the absorbed N from the forage feeds, which may relate to the absorbed AA-N composition relative to AA-N in milk protein in addition to the relative amounts of AA-N and non-protein N produced by each feed. Significant differences in parameter estimates between feeds point to some differentiation in both digestion and metabolism dynamics between feeds

and feed types (i.e., forage vs. concentrates). However, results varied with the form of excretion and phase of experiment modeled. Future elucidation of the kinetics of N digestion and metabolism requires further refinement of the excretion pools, including microbial and rumen-undegraded N, milk urea N, and purine derivative and creatinine N in urine. Future experimental work in this area should also design sampling with varying time between samples and include experimental periods greater than 80 h after the cessation of labeled feeding to capture the information needed to describe additional pools.

NOTES

Partial funding for the study was received from USDA Agricultural Research Services (Washington, DC) grant no. 58-3655-4-049, NIFA award no. 2015-08601, and USDA Hatch project nos. WIS 01660, WIS01725, WIS01892, and WIS05009. Mention of any trademark or proprietary product in this paper does not constitute a guarantee or warranty of the product by the USDA or the Agricultural Research Service and does not imply its approval to the exclusion of other products that also may be suitable. The University of Wisconsin–Madison (Madison, WI) Institutional Animal Care and Use Committee approved all study procedures. The authors have not stated any conflicts of interest.

Nonstandard abbreviations used: ΔAPE = change in APE; AA-N = blood AA N; A_i = asymptotic APE; ANA = above natural abundance; AP = atom percent; APE = atom percent excess; APE_{Ini} = APE from dietary intake; AR-1 = first-order autoregressive; AS = ^{15}N-labeled alfalfa silage; CG = ^{15}N-labeled corn grain; CS = ^{15}N-labeled corn silage; ED = error due to random dispersion; FN = fecal N; FPCM = fat- and protein-corrected milk; *k* = rate of turnover; L = lag time; M1 = enrichment phase model; M2 = decay phase model; M3 = model of both enrichment and decay phases; MCP = microbial crude protein; MN = milk N; NASEM = National Academies of Science, Engineering, and Medicine; NUUN = nonurea urinary N; RMSE = root mean square error; SBM = ^{15}N-labeled soybean meal; UN = urine N; UUN = urinary urea N.

REFERENCES

Barros, T., J. M. Powell, M. A. C. Danes, M. J. Aguerre, and M. A. Wattiaux. 2017. Relative partitioning of N from alfalfa silage, corn silage, corn grain, and soybean meal into milk, urine, and feces, using stable ^{15}N isotope. Anim. Feed Sci. Technol. 229:91–96. https://doi.org/10.1016/j.anifeedsci.2017.05.009.

Bequette, B. J., J. A. Metcalf, D. Wray-Cahen, F. R. C. Backwell, J. D. Sutton, M. A. Lomax, J. C. Macrae, and G. E. Lobley. 1996. Leucine and protein metabolism in the lactating dairy cow mammary gland: Responses to supplemental dietary crude protein intake. J. Dairy Res. 63:209–222. https://doi.org/10.1017/S002202990003171X.

Bibby, J., and H. Toutenburg. 1977. Prediction and Improved Estimation in Linear Models. John Wiley and Sons, London, United Kingdom.

Brooks, P. D., J. M. Stark, B. B. McInteer, and T. Preston. 1989. Diffusion method to prepare soil extracts for automated nitrogen-15 analysis. Soil Sci. Soc. Am. J. 53:1707–1711. https://doi.org/10.2136/sssaj1989.03615995005300060016x.

Cantalapiedra-Hijar, G., I. Ortigues-Marty, B. Sepchat, J. Agabriel, J. F. Huneau, and H. Fouillet. 2015. Diet-animal fractionation of nitrogen stable isotopes reflects the efficiency of nitrogen assimilation in ruminants. Br. J. Nutr. 113:1158–1169. https://doi.org/10.1017/S0007114514004449.

Cantalapiedra-Hijar, G. H., C. Fouillet, C. Chantelauze, N. Khodorova, L. Bahloul, and I. Ortigues-Marty. 2020. The isotopic nitrogen turnover rate as a proxy to evaluate in the long-term the protein turnover in growing ruminants. J. Agric. Sci. 157:701–710. https://doi.org/10.1017/S0021859620000118.

Dijkstra, J., J. France, and S. Tamminga. 1998. Quantification of the recycling of microbial nitrogen in the rumen using a mechanistic model of rumen fermentation processes. J. Agric. Sci. 130:81–94. https://doi.org/10.1017/S0021859697004929.

Dijkstra, J., O. Oenema, J. W. van Groenigen, J. W. Spek, A. M. van Vuuren, and A. Bannink. 2013. Diet effects on urine composition of cattle and N_2O emissions. Animal 7:292–302. https://doi.org/10.1017/S1751731113000578.

Gustafsson, A. H., and D. L. Palmquist. 1993. Diurnal variation of rumen ammonia, serum urea, and milk urea in dairy cows at high and low yields. J. Dairy Sci. 76:475–484. https://doi.org/10.3168/jds.S0022-0302(93)77368-3.

Hothorn, T., F. Bretz, and P. Westfall. 2008. Simultaneous inference in general parametric models. Biom. J. 50:346–363. https://doi.org/10.1002/bimj.200810425.

INRA. 2018. INRA Feeding System for Ruminants. Wageningen Academic Publishers. Wageningen, the Netherlands.

Lapierre, H., R. Martineau, M. D. Hanigan, H. J. van Lingen, E. Kebreab, J. W. Spek, and D. R. Ouellet. 2020. Review: Impact of protein and energy supply on the fate of amino acids from absorption to milk protein in dairy cows. Animal 14 (Suppl. 1):s87–s102. https://doi.org/10.1017/S1751731119003173.

Lapierre, H., D. R. Ouellet, R. Berthiaume, R. Martineau, G. Holtrop, and G. E. Lobley. 2008. Distribution of ^{15}N in amino acids during ^{15}N-leucine infusion: Impact on the estimation of endogenous flows in dairy cows. J. Dairy Sci. 91:2702–2714. https://doi.org/10.3168/jds.2007-0871.

Leterme, P., W.-B. Souffrant, and A. Théwis. 2000. Effect of barley fibres and barley intake on the ileal endogenous nitrogen losses in piglets. J. Cereal Sci. 31:229–239. https://doi.org/10.1006/jcrs.2000.0306.

Lobley, G. E. 2003. Protein turnover—What does it mean for animal production? Can. J. Anim. Sci. 83:327–340. https://doi.org/10.4141/A03-019.

Marini, J. C., D. G. Fox, and M. R. Murphy. 2008. Nitrogen transactions along the gastrointestinal tract of cattle: A meta-analytical approach. J. Anim. Sci. 86:660–679. https://doi.org/10.2527/jas.2007-0039.

NASEM (National Academies of Sciences, Engineering, and Medicine). 2021. Nutrient Requirements of Dairy Cattle. 8th rev. ed. National Academies Press. Washington, DC.

NRC (National Research Council). 2001. Nutrient Requirements of Dairy Cattle. 7th rev. ed. National Academies Press, Washington, DC.

Ouellet, D. R., M. Demers, G. Zuur, G. E. Lobley, J. R. Seoane, J. V. Nolan, and H. Lapierre. 2002. Effect of dietary fiber on endogenous nitrogen flows in lactating dairy cows. J. Dairy Sci. 85:3013–3025. https://doi.org/10.3168/jds.S0022-0302(02)74387-7.

Pinheiro, J., D. Bates, S. DebRoy, and D. Sarkar. 2017. nlme: Linear and nonlinear mixed effects models. R package version 3.1-131. Accessed Feb. 15, 2018. https://CRAN.R-project.org/package=nlme.

Powell, J. M., T. Barros, M. A. C. Danes, M. J. Aguerre, M. A. Wattiaux, and K. F. Reed. 2017. Nitrogen use efficiencies to grow, feed, and recycle manure from the major diet components fed to dairy cows in

the USA. Ag., Ecosyst., and Environ. 239:274–282. https://doi.org/10.1016/j.agee.2017.01.023.
Powell, J. M., K. A. Kelling, G. R. Munoz, and P. R. Cusick. 2005. Evaluation of dairy manure nitrogen-15 enrichment methods on short-term crop and soil nitrogen budgets. Agron. J. 97:333–337. https://doi.org/10.2134/agronj2005.0333.
Powell, J. M., and C. A. Rotz. 2015. Measures of nitrogen use efficiency and nitrogen loss from dairy production systems. J. Environ. Qual. 44:336–344. https://doi.org/10.2134/jeq2014.07.0299.
Reed, K. F., D. P. Casper, J. France, and E. Kebreab. 2015. Prediction of nitrogen efficiency in dairy cattle: A review. Perspect. Agric. Vet. Sci. Nutr. Nat. Resour. 10:1–12. https://doi.org/10.1079/PAVSNNR201510001.
Spek, J. W., J. Dijkstra, G. van Duinkerken, W. H. Hendriks, and A. Bannink. 2013. Prediction of urinary nitrogen and urinary urea nitrogen excretion by lactating dairy cattle in northwestern Europe and North America: A meta-analysis. J. Dairy Sci. 96:4310–4322. https://doi.org/10.3168/jds.2012-6265.
Strathe, A. B., A. Danfær, H. Sørensen, and E. Kebreab. 2010. A multilevel nonlinear mixed-effects approach to model growth in pigs. J. Anim. Sci. 88:638–649. https://doi.org/10.2527/jas.2009-1822.
Wattiaux, M. A., and J. D. Reed. 1995. Fractionation of nitrogen isotopes by mixed ruminal bacteria. J. Anim. Sci. 73:257–266. https://doi.org/10.2527/1995.731257x.

ORCIDS

Kristan F. Reed https://orcid.org/0000-0003-1766-4148
MaryGrace Erickson https://orcid.org/0000-0002-8919-2664
Marina A. C. Danes https://orcid.org/0000-0003-4196-8328
Geoffrey I. Zanton https://orcid.org/0000-0002-6946-540X
Michel A. Wattiaux https://orcid.org/0000-0001-8713-1641

APPENDIX

APPENDIX 1

Model Structure

In Equation A1,

$$y_{ij} = \mathbf{X}_i\boldsymbol{\beta}_i + \varepsilon_{ij}, \quad [A1]$$

y_{ij} is the APE observation from 1 of 3 exit pools at the jth time point from cows fed the ith diet for j = 1, 2, 3,…29 and i = 1, 2, 3, 4; $\mathbf{X}_i$ is the 1 × 2 covariate matrix with 1 column for the intercept and 1 column for time in hours after feeding (t = 0 to 176 h) for the ith diet; $\boldsymbol{\beta}_i$ is the 2 × 1 vector of parameter estimates for the intercept and relationship of dependent variable with time for the ith diet; and ε_{ij} are the residual errors of the jth observation from the ith diet which are assumed to follow a normal distribution with a mean of 0 and common residual variance of σ^2.

Models for Equation A1 were fit with the lm() function in the stats package in R statistical software. Inclusion of higher order terms (e.g., t^2) was considered, but there is often no biological interpretation of polynomial parameters. Because the objective of this study was not prediction, higher order models of the transformed data were not investigated.

Exponential Models of Rise and Decay Curves

Next, a single-pool exponential model was fit separately to the rise and decay datasets where the dataset for the rising curve model (Equation A2) was truncated at 96 h after initiation of labeled feeding and the dataset for the decaying curve model (Equation A3) started at 96 h after labeled feeding. The timepoints in the dataset for the decaying curve model were adjusted to start at 0 h such that the first observations of FN and UN APE in the decaying curve dataset were at t = 2 h and the first observation of MN APE was at t = 8 h. The models for the data were as follows:

$$y_{ij} = \begin{cases} 0 & t_j < L_{1i} \\ A_i - A_i e^{-k_i(t_j - L_{1i})} & t_j \geq L_{1i} \end{cases} \quad [A2]$$

and

$$y_{ij} = \begin{cases} A_i & t_j < L_{1i} \\ A_i e^{-k_i(t_j - L_{1i})} & t_j \geq L_{1i} \end{cases}, \quad [A3]$$

where y_{ij} is an APE observation from 1 of 3 exit pools from the ith diet at the jth time point; A_i is the estimated asymptotic plateau of APE for the ith diet; k_i is the estimated rate of exponential decay of the ith diet towards the plateau (Equation A2) or toward 0 (Equation A3); t_j is the jth time point from either the initiation of labeled feeding or the start of the decay phase (96 h after start of labeled feeding); and L is the estimated lag time in hours from t = 0 h until the rise or decay begins. Models were fit in R statistical software using the nlme function in the stats package.

Piecewise Nonlinear Model

A piecewise non-linear model with parameter sharing was developed to utilize data from both the rise and decay as a function of time (t) was fit from t = 0 h until t = 176 h:

$$y_{ij} = \begin{cases} 0 & t_j < L_{1i} \\ A_i - A_i e^{-k_i(t_j - L_{1i})} & L_{1i} < t_j < L_{1i} + L_2 \\ \hat{A}_{(t)i} e^{k_i(t_j - (L_{1i} + L_2))} & L_{1i} + L_2 < t_j \end{cases}, \quad [A4]$$

where, y_{ij} is the APE of exit pools from cows fed diet i at time point t_j; A_i is estimated maximum APE of exit pools from a cow fed diet i; $\hat{A}_{(t)i}$ is the estimated APE of exit pools from a cow fed diet i at the timepoint $t = L_1 + L_2$; k_i is fractional rate of APE accumulation or decay for the ith diet; L_{1i} is the lag from time $t = 0$ to the time when APE begins to increase in exit pools for the jth diet; L_{2i} is the lag from time $t = L_{1i}$ to $t = (L_{1i} + L_{2i})$ when APE of the exit pools from the ith diet begins to decay from the maximum APE during the experimental period. Heuristically, L_2 is the amount of time the labeled diet was fed.

APPENDIX 2

Stochastic Structure

The overall structure of the model is as follows:

$$y_{ijk} = f(\boldsymbol{\theta}_{ij}, t_{ijk}) + \boldsymbol{\varepsilon}_{ijk}, \quad [A5]$$

where $f(\boldsymbol{\theta}_{ij}, t_{ijk})$ represents the mean function described in M1–3 (Table 2; Equations A2, A3, and A4; $\boldsymbol{\theta}_{ij}$ is the set of parameters required for the mean function; t_{ijk} is the kth time-point; and $\boldsymbol{\varepsilon}_{ijk}$ is the random error. Both $\boldsymbol{\theta}$ and $\boldsymbol{\varepsilon}$ were built sequentially to include random components with increasing complexity. Initially, $\boldsymbol{\theta}$ was a vector of only fixed effects consisting of the product of the matrix of all possible fixed effects and the diet indicator vector:

$$\boldsymbol{\theta}_{ij} = \begin{bmatrix} \beta_{11} & \cdots & \beta_{14} \\ \vdots & \ddots & \vdots \\ \beta_{1l} & \cdots & \beta_{4l} \end{bmatrix} \begin{bmatrix} x_{1ij} \\ x_{2ij} \\ x_{3ij} \\ x_{4ij} \end{bmatrix}, \quad [A6]$$

where β_{il} is the lth fixed effect parameter for diet i and x_{ijl} are the indicator variables for the jth animal on the ith diet for parameter l. The baseline error structure for $\boldsymbol{\varepsilon}$ was

$$\varepsilon_{ijk} = \begin{bmatrix} \varepsilon_{ij1} \\ \vdots \\ \varepsilon_{ijn} \end{bmatrix} \sim N\left(0, \sigma^2 \boldsymbol{\omega}\right), \quad [A7]$$

where σ^2 is the variance and $\boldsymbol{\omega}$ is the n × n (k =1,…, n) identity matrix indicating $\boldsymbol{\varepsilon}_{ijk}$ are independent and identically distributed.

Because N efficiency and rates of excretion are expected to vary with animal, the first increase in the random structure complexity was to add an additive random animal effect to each parameter such that

$$\theta_{ij} = \begin{bmatrix} \beta_{11} & \cdots & \beta_{14} \\ \vdots & \ddots & \vdots \\ \beta_{1l} & \cdots & \beta_{4l} \end{bmatrix} \begin{bmatrix} x_{1ij} \\ x_{2ij} \\ x_{3ij} \\ x_{4ij} \end{bmatrix} + \begin{bmatrix} b_{ij}^{(1)} \\ \vdots \\ b_{ij}^{(l)} \end{bmatrix}. \quad [A8]$$

For example, the first parameter for the exponential rise model (M1) would be

$$A_{ij} = \beta_{11} x_{11j} + \beta_{12} x_{12j} + \beta_{13} x_{13j} + \beta_{14} x_{14j} + b_{ij}^{(l)}, \quad [A9]$$

where $b_{ij}^{(l)}$ is the random effect for the lth parameter and is distributed as

$$\begin{bmatrix} b_{ij}^{(1)} \\ \vdots \\ b_{ij}^{(l)} \end{bmatrix} \sim N\left(0, \varphi_{ij}\right), \varphi_{ij} = \begin{bmatrix} \varphi_{ijl} & \cdots & 0 \\ \vdots & \ddots & \vdots \\ 0 & \cdots & \varphi_{ijl} \end{bmatrix}, \quad [A10]$$

and φ_{ijl} is the random effect of the jth animal fed diet i for the lth fixed effect in the model.

Next, because the experimental design included repeated measures, a first order autoregressive (**AR-1**) covariance structure was added by changing the ω from the identity matrix in the baseline error structure to a standard AR-1 covariance matrix:

$$\boldsymbol{\omega}_{ij} = \frac{1}{1 - \rho_{ij}^2} \begin{bmatrix} 1 & \rho^{ij} & 0 & 0 \\ \rho^{ij} & 1 & \cdots & \rho^{ij} \\ 0 & \vdots & \rho^{ij} & 1 \end{bmatrix}, \quad [A11]$$

where $\boldsymbol{\omega}_{ij}$ is the n × n matrix that when multiplied by σ^2 defines the covariance matrix $\boldsymbol{\varepsilon}_{ij}$, and ρ_{ij} is the autocorrelation parameter estimating the degree of correlation between observation from the same animal on the same diet at time t_k and t_{k+1}.

The final addition to the model random structure was to include a weighted covariance matrix that gives additional weight to observations from the beginning and end of the trial periods because these APE values were very close to zero. For this model, the covariance matrix is the product of the AR-1 matrix and the weighted matrix so $\boldsymbol{\omega} = \boldsymbol{\omega}_1 \boldsymbol{\omega}_2$, where $\boldsymbol{\omega}_1$ is the AR-1 matrix described in Equation 11 and $\boldsymbol{\omega}_2$ is defined as

$$\boldsymbol{\omega}_2 = \begin{Bmatrix} \frac{1}{\left(\overline{y}_{i,k} + 0.1\right)} & \cdots & 1 \\ \vdots & \ddots & \vdots \\ 1 & \cdots & \frac{1}{\left(\overline{y}_{i,k} + 0.1\right)} \end{Bmatrix}, \quad [A12]$$

where $\bar{y}_{i,k}$ is the average APE for time point t_{ik}.

APPENDIX 3

Method to Estimate the Proportion of Excreted N from Each Feed

1. Given the assumption that the ^{15}N over that which occurs at natural abundance (NA) is from the labeled feed, let $prop_i$ be the proportion of N in the exit pool that is from the labeled feed i.

- The following formula establishes the relationship between the feed ^{15}N atom percent (AP_{Feed}) and the exit pool AP (AP_{Ex}):

$$AP_{Ex} = prop_i \times AP_{Feed_i} + \left(1 - prop_i\right) \times NA.$$

2. After rearrangement of the above to solve for $prop_i$, we find,

$$prop_i = \frac{AP_{Ex} - NA}{AP_{Feed_i} - NA} = \frac{APE_{Ex}}{APE_{Feed_i}}.$$

APPENDIX 4

Descriptions of Assumptions for Estimation of N Excretion from Individual Feeds with NRC (2001) and NASEM (2021) Models

NRC (2001). The following assumptions were employed to arrive at the proportion of feed N in each exit pool. First, RDP, RUP, MCP, MP, and endogenous protein are sourced from the modeled feed in proportion to diet composition. Second, undigested non-protein endogenous N is excreted in feces. Third, 60% of the RDP balance is excreted in urine and 40% is excreted in feces. While other nutrient requirement systems such as the INRA feeding system provide explicit estimates of this value (INRA, 2018), the NRC is unclear as to the fate of protein fractions A and B that are degraded in the rumen but not used for MCP. For the final assumption, we explored the impact of the proportion of RDP balance excreted in urine on total UN and FN estimates. A simple sensitivity analysis was conducted to assess how the estimate for the proportion of RDP balance that is allocated to urine and feces affects the NRC estimates of total fecal and urinary N excretion (depicted here as urine and fecal CP excretion; Appendix 6, Figure A1, A2). The points represent the NRC (2001) estimates of total urinary and fecal CP excretion using animal and dietary inputs from the 4 treatment means as described in the Methods. The green line represents the overall experimental average urinary and fecal CP excretion from Equations 1 and 2 from Reed et al (2015), respectively. Similarly, the dark blue lines are the values predicted for the experimental average fecal and urinary CP excretion by CNCPS v. 6.5 (Cornell University). The light blue line is the experimental average value of the excreted fecal and urinary CP.

Based on the results of the total collection, both the models from Reed et al. (2015) and CNCPS v. 6.5 over predict fecal N. Reed et al. (2015) over predicts UN, as well. However, the total collection can be assumed to be an underestimate of true excretion (especially due to possible lost excretion en route to the parlor). The partition value of 0.6 was selected as a value that predicts UN and fecal N slightly above the measured values from this study's total collection (Barros et al., 2017) and closer to the predicted values for fecal N. By comparison, the value of 0.79 proposed by the INRA feeding system would have resulted in predicted urinary CP values close to those estimated by the equations of Reed et al. (2015), but a further over prediction of the urinary CP in comparison to our selected value of 0.6, and under prediction of the fecal CP.

NASEM (2021). Undigested protein fractions were allocated to FN. In addition, a 3-step procedure was developed to allocate digested feed protein (MP and RDP balance) to exit pools. First, supplies of individual EAA_a (a = Arg, His, Ile…Val) in MP were allocated to exit EAA pools (fecal endogenous, urinary endogenous, and milk) in proportion to the relative demands of each exit pool for each EAA_a. The efficiencies of MP use and CP-to-N conversion factors were specific to each EAA_a. Supplies of EAA_a in excess of body recommended flows were carried forward to meet total NEAA requirements. The use of individual EAA_a for a feed ingredient (i = AS, CS, CG, SBM) was determined using the ratio of EAA_a supplied by feed i to the EAA_a supplied by the diet. Second, residual MP consisted of the MP not used to meet body EAA and NEAA requirements in step 1. Residual MP was allocated to exit pools in proportion to the predicted demands for NEAA in fecal endogenous, urinary endogenous, and milk net protein. In contrast to step 1, step 2 used a scalar MP-use efficiency (0.69) and N/CP conversion factors (6.25, except milk = 6.34). The supplies of residual MP that exceeded recommended body and flows of EAA and NEAA were carried forward as residual circulating N in the subsequent step. The use of residual MP for a feed (i = AS, CS, CG, SBM) was computed using the ratio of residual MP supplied by feed i to the residual MP supplied by the diet. Third, residual circulating N consisted of the residual MP not used in step 2 plus the RDP balance. Residual circulating N was allocated to meet recommended flows of fecal endogenous NPN, urinary endogenous NPN, and milk NPN. Circulating N was assumed to meet NPN predicted flows with an efficiency of 1.0. Residual circulating N in excess of NPN recommended flows was

allocated to urine. The use of residual N for a feed (i = AS, CS, CG, SBM) was calculated using the ratio of residual N supplied by feed i to the residual N supplied by the diet. Notably, compared with NRC (2001), the NASEM (2021) model estimates reflect not only updates to the model, but also revisions to the feed library values.

APPENDIX 5

Table A1. Kinetic parameter estimates (SE) of ^{15}N enrichment in fecal N, urinary N, urinary urea N, and milk N for enrichment (M1), decay (M2), and piecewise enrichment and decay (M3) models[1]

			Treatment[2]				
Excretion	Parameter	Model	AS	CS	CG	SBM	P-value[3]
Fecal N	A (%)	M1	0.248 (0.0052)	0.201 (0.0053)	0.123 (0.0069)	0.168 (0.0060)	<0.001
		M2	0.243 (0.0081)	0.188 (0.0082)	0.119 (0.0099)	0.169 (0.0098)	<0.001
		M3	0.254 (0.0035)	0.197 (0.0032)	0.124 (0.0042)	0.180 (0.0042)	<0.001
	k, h^{-1}	M1	0.0582 (0.00426)	0.0537 (0.00486)	0.0417 (0.00746)	0.0460 (0.00538)	
		M2	0.0383b (0.00346)	0.0629a (0.00646)	0.0335b (0.00499)	0.0290b (0.00338)	<0.01
		M3	0.0436ab (0.00309)	0.0623a (0.00477)	0.0394b (0.00537)	0.0332b (0.00354)	<0.05
	L_1, h	M1	17.8a (0.625)	11.0b (0.878)	10.6b (1.91)	12.8b (1.62)	
		M2	15.2ab (1.30)	17.8a (0.924)	11.3ab (2.86)	10.9b (2.30)	<0.05
		M3	12.9ab (0.713)	13.2a (0.677)	10.2ab (1.89)	8.92b (1.54)	<0.10
	L_2, h	M3	95.4 (0.663)				
Urinary N	A	M1	0.180 (0.0036)	0.123 (0.0033)	0.104 (0.0047)	0.156 (0.0029)	<0.001
		M2	0.195 (0.0047)	0.136 (0.0045)	0.133 (0.0046)	0.198 (0.0041)	<0.001
		M3	0.167 (0.0024)	0.120 (0.0026)	0.101 (0.0028)	0.161 (0.0025)	<0.001
	k, h^{-1}	M1	0.0357 (0.00345)	0.0407 (0.00518)	0.0324 (0.00541)	0.0430 (0.00386)	
		M2	0.0397a (0.00161)	0.0375ab (0.00182)	0.0377ab (0.00196)	0.0331b (0.00134)	<0.05
		M3	0.0457 (0.00257)	0.0446 (0.00350)	0.0388 (0.00350)	0.0395 (0.00213)	
	L_1, h	M1	4.70 (0.913)	3.16 (1.41)	4.64 (1.78)	6.36 (0.811)	
		M2	NA				
		M3	5.13 (0.689)	4.52 (0.956)	6.16 (1.10)	6.79 (0.681)	
	L_2, h	M3	94.5 (0.604)				
Urinary urea N	A	M1	0.203 (0.0034)	0.133 (0.0032)	0.109 (0.0046)	0.172 (0.0029)	<0.001
		M2	0.230 (0.0072)	0.154 (0.0069)	0.144 (0.0066)	0.234 (0.0065)	<0.001
		M3	0.190 (0.0032)	0.132 (0.0033)	0.109 (0.0034)	0.181 (0.0034)	<0.001
	k, h^{-1}	M1	0.0405 (0.00384)	0.0462 (0.00602)	0.0369 (0.00622)	0.0486 (0.00440)	
		M2	0.0437a (0.00200)	0.0404ab (0.00266)	0.0373ab (0.00254)	0.0359b (0.00149)	<0.05
		M3	0.0493 (0.00246)	0.0457 (0.00342)	0.0399 (0.00314)	0.0428 (0.00197)	
	L_1, h	M1	5.14 (0.819)	3.32 (1.38)	5.49 (1.69)	6.90 (0.743)	
		M2	NA				
		M3	5.16b (0.589)	3.88b (0.932)	6.56ab (0.986)	7.32a (0.575)	
	L_2, h	M3	94.3 (0.557)				

Continued

Table A1 (Continued). Kinetic parameter estimates (SE) of ^{15}N enrichment in fecal N, urinary N, urinary urea N, and milk N for enrichment (M1), decay (M2), and piecewise enrichment and decay (M3) models[1]

			Treatment[2]				
Excretion	Parameter	Model	AS	CS	CG	SBM	*P*-value[3]
Milk N	A	M1	0.137 (0.0075)	0.106 (0.0057)	0.124 (0.0085)	0.182 (0.0043)	<0.001
		M2	0.154 (0.0068)	0.122 (0.0070)	0.133 (0.0072)	0.199 (0.0067)	<0.001
		M3	0.129 (0.0044)	0.105 (0.0043)	0.107 (0.0044)	0.184 (0.0044)	<0.001
	k, h^{-1}	M1	0.0252 (0.00462)	0.0271 (0.00463)	0.0204 (0.00399)	0.0296 (0.00320)	
		M2	0.0266 (0.00132)	0.0277 (0.00176)	0.0290 (0.00171)	0.0255 (0.000970)	
		M3	0.0285 (0.00183)	0.0286 (0.00200)	0.0303 (0.00213)	0.0279 (0.00159)	
	L_1, h	M1	10.5 (2.02)	6.47 (1.51)	6.31 (1.64)	6.93 (0.782)	
		M2	NA				
		M3	10.2a (0.922)	7.30ab (0.971)	9.80a (1.08)	6.61b (0.591)	<0.05
	L_2, h	M3	92.1 (0.733)				

[a,b]Means within a row that do not share a common letter superscript are different ($P < 0.10$).

[1]Asymptotic atom percent excess (A) and rate constants (k) are presented for all models. Lag parameters (L_1 and L_2) for M2 were omitted for urinary N, urinary urea N, and milk N because model fits suggested lag time was zero.

[2]Dietary treatments: AS = ^{15}N-labeled alfalfa silage; CS = ^{15}N-labeled corn silage; CG = ^{15}N-labeled corn grain; SBM = ^{15}N-labeled soybean meal.

[3]*P*-values provided refer to the smallest possible cutoff (0.001, 0.01, 0.05, or 0.10) for all possible comparisons of parameter estimates between diets.

APPENDIX 6

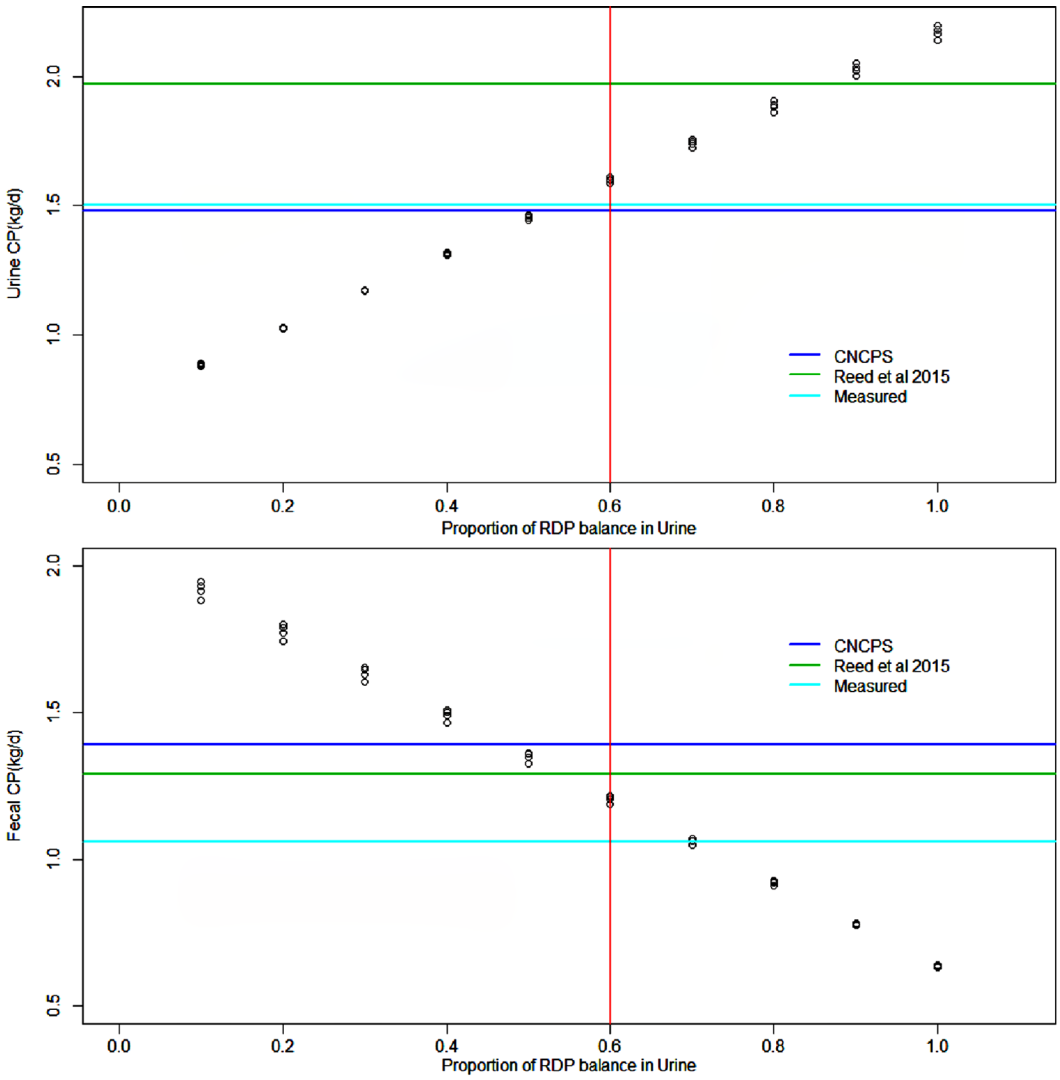

Figure A1. Graphical depiction of sensitivity analysis to estimate proportion of RDP balance allocated to feces and urine in NRC (2001) nutrient requirement model. Points represent NRC (2001) estimates of total urinary and fecal CP for different values of the proportion of RDP balance in each. The light blue lines are the average measured values of fecal and urinary CP; the green lines are the average values estimated by Reed et al. (2015); and the dark blue lines are the average values estimated by CNCPS v. 6.5.

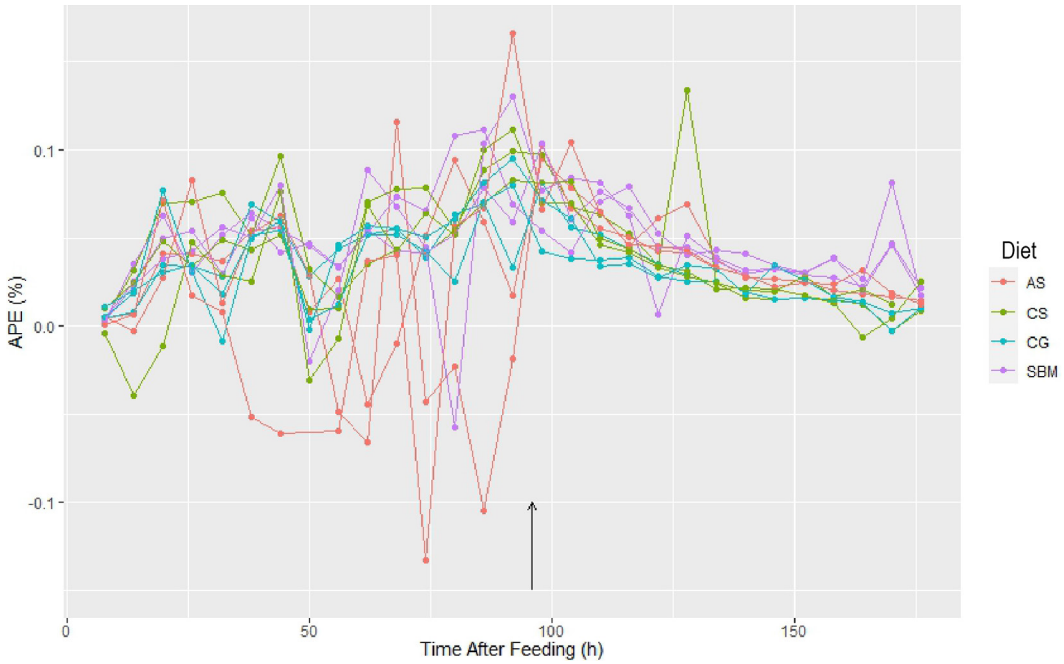

Figure A2. Non-urea urinary nitrogen atom percent excess (APE, %) for diets with labeled alfalfa silage (AS), corn silage (CS), corn grain (CG), and soybean meal (SBM). Each point represents 1 of 3 individual cow observations per time point, with lines connecting observations within cow. Arrow indicates time of last labeled feeding.